Food Chemistry: X 22 (2024) 101511

Contents lists available at ScienceDirect

Food Chemistry: X

journal homepage: www.sciencedirect.com/journal/food-chemistry-x

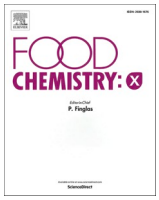

# Effect of *Cyperus esculentus* polysaccharide on *Cyperus esculentus* starch: Pasting, rheology and *in vitro* digestibility

Xiuli Wu [*,1], Qing Zhang [1], Jianwen Zhang [1], Bingqian Zhang [1], Xuexu Wu [1], Xiangxuan Yan [1]

*College of Food Science and Engineering, Changchun University, Changchun 130022, Jilin, China*

ARTICLE INFO

*Keywords:*
*Cyperus esculentus* starch-polysaccharide complexes
Pasting
Rheological
*In vitro* digestibility

ABSTRACT

This study investigated the effects of varying amounts of added *Cyperus esculentus* polysaccharide (CEP) on the physicochemical and structural properties, as well as *in vitro* digestibility, of homologous *Cyperus esculentus* starch (CES). Compared to CES, the CES-CEP complexes showed reduced peak viscosity and breakdown value, and improved thermal paste stability of starch. Rheological properties showed that adding CEP reduced the consistency coefficient and pseudoelasticity of the complexes, thus increasing their resistance to shear thinning. FTIR analysis suggested the absence of covalent binding between CES and CEP. SEM showed a more homogeneous and dense gel structure, particularly in the CES-1.0%CEP sample. During *in vitro* digestion, the content of resistant starch in the complexes increased after CEP was added. Analysis of the interaction forces showed that the CES-CEP complexes had stronger hydrogen bonding and electrostatic interaction. This study offers valuable insights into the potential applications of CEP in starch-based foods.

## 1. Introduction

*Cyperus esculentus* (*C. esculentus*) is a non-grain economic crop that can offer a range of products, including oil, grains, forage, and grass. Its rich content of starch (23–37%), oil (19–41%), and polysaccharides (13–18%) often makes it a promising raw material for the food industry (Zhang et al., 2023). However, with the continuous development of the industrialization of *C. esculentus*, there is still about 38.39–62.71% of starch in the *C. esculentus* meal that is not effectively utilised, and the comprehensive utilization of this part of the by-products will maximise the value of the *C. esculentus*. *C. esculentus* starch (CES) contains a high content of amylose (25%) and exhibits rheological properties similar to corn and potato starch. However, its gel structure properties, such as hardness, springiness, adhesiveness, and chewiness, are superior to those of corn and potato starch (Builders, Anwunobi, Mbah, & Adikwu, 2013). Therefore, CES has great potential as a food thickener, fat replacer, stabiliser, and gelatiniser in the food industry.

However, due to the inherent limitations of native starch, such as its susceptibility to retrogradation and poor stability, which limit the application of CES in the food industry, starch modification is necessary. The combination of polysaccharides and starch is an excellent physical modification method. This approach is relatively simple, cost-effective, and environmentally friendly, serving as an alternative to chemical modification or other expensive physical modification methods (Xiao et al., 2020). Liu et al. (2018) found that *Mesona chinensis* polysaccharide can enhance the thermal stability of wheat starch during the initial stage of gelatinization, improving its rheological properties. Konjac glucomannan can inhibit the swelling of starch granules, significantly altering the pseudoplasticity and viscoelasticity of corn starch (Ma, Zhu, Wang, Wang, & Wang, 2019). Existing research has shown that CES can interact with Chinese quince seed gum, enhancing the freeze-thaw stability, viscosity, and pseudoplasticity of the gel (Liu et al., 2021).

*C. esculentus* polysaccharide (CEP) is a water-soluble polysaccharide primarily composed of glucose, mannose, galactose and rhamnose, of which glucose is the dominant component. CEP has a linear chain and branched chains containing a variety of functional groups, which can inhibit the generation of free radicals, enhance the activity of antioxidant enzymes, and improve the antioxidant capacity (Hernández-Olivas et al., 2022). It also has the advantages of lowering blood lipids and regulating immunity (Yu et al., 2023). Moreover, the regulation of blood glucose by CEP has received widespread attention. Currently, relevant

* Corresponding author.
*E-mail addresses:* wuxl@ccu.edu.cn (X. Wu), 230301116@mails.ccu.edu.cn (Q. Zhang), 220302133@mails.ccu.edu.cn (J. Zhang), 230301114@mails.ccu.edu.cn (B. Zhang), 220302127@mails.ccu.edu.cn (X. Wu), 220301081@mails.ccu.edu.cn (X. Yan).
[1] Changchun University, Changchun, Jilin Province 130022, China.

https://doi.org/10.1016/j.fochx.2024.101511
Received 29 March 2024; Received in revised form 24 May 2024; Accepted 24 May 2024
Available online 29 May 2024

studies on CEP primarily focus on the physicochemical properties, interactions with proteins and biological activities of CEP.

There are fewer studies on the physicochemical properties of CEP in CES. Therefore, in this experiment, different amounts of CEP were used to prepare CES-CEP complexes, and their functional properties such as pasting, rheological properties and *in vitro* digestion were investigated. The mechanism of the interaction between CEP and CES in the complexes was explored to provide a theoretical basis for the addition of CEP as a functional ingredient in starch-rich foods.

## 2. Materials and methods

### 2.1. Materials

The *C. esculentus* was purchased from Hefei Zhoudao Food Co., Ltd. (Anhui, China). α-Amylase (CAS#9000-90-2, 50 U/mg from hog pancreas) was purchased from Sigma-Aldrich Co. (St Louis, MO, USA). *Amyloglucosidase* (CAS#9032-08-0, 10,000 U/mL from *Aspergillus niger*) was purchased from Shanghai Macklin Biochemical Co. Ltd. (Shanghai, China). All other chemicals were of analytical purity grade.

### 2.2. Extraction of CES and CEP

The extraction of CES and CEP is shown in Fig. S1. Briefly, 100 g of *C. esculentus* meal was mixed with 1.5 L of deionised water, adjusted the pH to 8.5, and stirred for 3 h. The mixture was sieved to 300 mesh and centrifuged at 3500 rpm for 20 min. The residue from the first centrifugation was taken to remove the upper grey impurities, the lower white starch was collected, and the water washing and centrifugation were repeated 3 times, dried and sieved through a 100 mesh sieve to obtain CES.

The supernatant of the first centrifugation was collected and centrifuged again to discard the lower protein residue (Isoelectric point method). Only the supernatant was collected, and the supernatant was rotary evaporated and ethanol-precipitation for 12 h. The residue was centrifuged and freeze-dried to obtain CEP.

### 2.3. Sample preparation

#### 2.3.1. Preparation of CES-CEP complexes

The method of Zhou et al. (2022) was referred to with minor modifications. 0.00, 0.03, 0.06, and 0.09 g of CEP were added to the dried CES for a total solids of 6 g, which were then dispersed in 100 mL of deionised water and mixed thoroughly to obtain the CES-0%CEP, CES-0.5%CEP, CES-1.0%CEP, and CES-1.5%CEP complexes.

#### 2.3.2. Preparation of CES-CEP freeze-dried complexes

Complexes were prepared by Section 2.3.1 samples were pasted in a boiling water bath for 30 min, cooled to room temperature freeze-dried, and then pulverised to obtain CES-CEP freeze-dried complexes.

### 2.4. Leaching of amylose

According to the method of Kong, Zhu, Zhang, and Zhu (2020), 0.1 g of CES-CEP complexes powder was prepared according to method Section 2.3.1. The samples were dispersed in 10 mL of deionised water and placed in a boiling water bath for 20 min. After cooling to room temperature, the samples were centrifuged at 3500 rpm for 30 min. 0.33 M NaOH solution (6 mL) was added to the supernatant. 0.1 mL of the above solution was taken and neutralised with 0.5% trichloroacetic acid solution. The samples were then stained by 0.01 M $I_2$-KI solution. Absorbance was measured at 620 nm with deionised water as the control. The content of leached amylose in the supernatant was calculated ($y = 0.0069\times$-$0.0730$, $R^2 = 0.9991$).

### 2.5. Solubility (S) and swelling power (SP)

The S and SP were evaluated using the method described by Jia et al. (2023). 0.2 g of CES-CEP complexes powder was placed in a centrifuge tube according to Section 2.3.1 and mixed with 10 mL of deionised water. The mixture was then heated at 80 °C for 30 min and cooled in an ice bath. Afterwards, the samples were centrifuged at 3000 rpm for 20 min. The resulting supernatant was collected and dried to a constant weight at 105 °C. The remaining precipitate was weighed and recorded. The S (%) was expressed as the weight ratio of the dried supernatant to the dry starch. The SP (g/g) was determined as the ratio of the wet weight of the precipitate to its dry weight. The S and SP were calculated as follows:

$$S(\%) = \frac{W_S}{W} \times 100\% \quad (1)$$

$$SP(g/g) = \frac{W_P}{W(1-S)} \quad (2)$$

where $W_S$ is the weight of the supernatant after drying (g); W is the weight of the dried sample (g); and $W_P$ is the weight of precipitation (g).

### 2.6. Pasting properties

Referring to the method of Zhou et al. (2022), a Brabender *v*iscometer (VISCOGRAPH-E, MELCHERS, Germany) was used to determine the viscosity of CES-CEP complexes. The steps were as follows:

Samples were prepared according to Section 2.3.1, 6% (dry basis, *w/v*) CES-CEP suspension was placed in a Brabender viscometer measuring cup. Temperature increased from 30 °C to 95 °C at 5 °C/min, held for 10 min, and then decreased to 50 °C at the same rate and held for 5 min. Viscosity measurements were also carried out by adding different concentrations of NaCl (0.2, 0.6, and 1.0 mol/L) and urea (0.2, 0.6, and 1.0 mol/L) to the CES-1.5%CEP complexes for determining the form of interacting forces in the CES-CEP complexes, which were determined as above.

### 2.7. Rheological measurements

#### 2.7.1. Steady shear rheological properties

Steady shear rheological properties of CES-CEP complexes were determined using a rotational rheometer (RHEOMETER RS3, BROOKFIELD, USA) following the method by Liu et al. (2023). The samples were prepared according to Section 2.3.1 and were pasted in a boiling water bath for 30 min, then immediately transferred to a rheometer. The shear rate ($\gamma$) was determined according to the following parameters: increasing from 0 to 300 $s^{-1}$ and then decreasing from 300 to 0 $s^{-1}$. The data obtained were fitted using the Ostwald-de Waele power-law equation:

$$\tau = K \times \gamma^n \quad (3)$$

where $\tau$ is the shear stress (Pa); K is the consistency coefficient (Pa·$s^n$); $\gamma$ is the shear rate ($s^{-1}$); *n* is the flow behaviour index (dimensionless).

#### 2.7.2. Dynamic rheological properties

The dynamic rheological properties of CES-CEP complexes were determined using a rotational rheometer (RSO, BROOKFIELD, USA) following the method by Liu et al. (2023). Samples were prepared according to Section 2.3.1. A 6% (dry basis, *w/v*) starch suspension was pasted in a boiling water bath for 20 min, then cooled to room temperature and transferred to the rheometer. A parallel probe (50 mm diameter, 1 mm gap) was used for dynamic rheological measurements. Sweep tests were carried out at 25 °C and in the frequency range of 0.1 to 10 Hz, with a strain value selected as 1%. The storage modulus (G') and loss modulus (G") were recorded.

### 2.8. Low-field nuclear magnetic resonance (LF-NMR)

The moisture distribution of the complexes was determined using an LF-NMR analyser (MESOMR-23-060H-I, NIUMAG ELECTRIC CORPORATION, Suzhou, China) using the method of Chen, Tian, Tong, Zhang, and Jin (2017). The CES-CEP complexes were prepared according to the method of Section 2.3.1, and the samples were placed in an NMR glass tube. The transverse relaxation time $T_2$ of the samples was measured using a CARR-PURCELL-MEIBOOM-GILL (CPMG) pulse sequence. The main parameters were set as follows: SF = 21 MHz, 01 = 143,395.68 Hz, TW = 1800 ms, NS = 16, and TE = 0.1000 ms. The signals were acquired using the NMRAS analysis software, and the data were inverted and normalised. Each sample was tested three times.

### 2.9. Fourier transform infrared (FTIR) spectroscopy

The infrared spectra of the samples were determined using an FTIR spectrometer (NICOLET IS5, Thermo Fisher, USA) following the method of Zhu et al. (2022). The samples were prepared according to the Section 2.3.2. The samples were mixed with KBr and ground and then pressed into thin slices. The wavenumbers ranged from 4000 to 400 $cm^{-1}$.

### 2.10. Scanning electron microscope (SEM)

SEM was determined using the method by Huang, Yu, Wang, and Shi (2023), CES-CEP complexes prepared according to Section 2.3.2 were fixed on the sample stage using conductive double-sided tape. After gold spraying, the samples were observed using SEM (JSM-6510LA, SHIMADZU CORPORATION, Japan). The magnifications used were 100× and 300×, with an accelerating voltage of 5 kV.

### 2.11. In vitro digestibility

The *in vitro* digestibility of samples was assessed with modifications to the method described by Jia et al. (2022). 0.2 g of samples were prepared by Section 2.3.1. Subsequently, 15 mL of 0.5 M sodium acetate buffer (pH 5.2) was added. The samples were pasted in a boiling water bath for 30 min, cooled to room temperature, and 10 mL of mixed enzyme solution containing α-amylase (290 U/mL) and glucosidase (180 U/mL) was added to the samples. Hydrolysates (1 mL) were taken at 0, 10, 20, 30, 60, 90, 120, 180, and 240 min. Then, 4 mL of anhydrous ethanol was added to inactivate the enzyme. Centrifugation was performed at 3000 rpm for 10 min, and the glucose content in the supernatant was measured using the DNS method.

$$RDS(\%) = \frac{0.9 \times (\rho_{20} - \rho_0) \times V}{m} \times 100 \quad (4)$$

$$SDS(\%) = \frac{0.9 \times (\rho_{120} - \rho_{20}) \times V}{m} \times 100 \quad (5)$$

$$RS(\%) = 100 - RDS(\%) - SDS(\%) \quad (6)$$

where $\rho_0$ is the free glucose mass before hydrolysis; $\rho_{20}$ and $\rho_{120}$ are the released glucose mass after 20 min and 120 min hydrolysis (mg/mL); $V$ is the total volume of the reaction system (mL); m is the total starch mass (mg).

The *in vitro* digestion curve of starch can be fitted to a first-order equation.

$$C_t = C_\infty \left(1 - e^{-kt}\right) \quad (7)$$

where $C_t$ is the amount of starch hydrolysed at t min; $C_\infty$ (%) is the estimated amount of starch digested at the end of digestion; k ($min^{-1}$) is the starch digestion rate constant.

### 2.12. Statistical analysis

Statistical analyses were performed using SPSS 26.0 and OMNIC software. The obtained data were statistically analysed by using one-way Analysis of Variance (ANOVA), and means were compared by Duncan's multiple range test ($p < 0.05$).

## 3. Results and discussion

### 3.1. Leaching of amylose

Leaching of amylose is a crucial parameter in the starch gelatinization process, which is generally exhibited as dilution and the inhibition of swelling (Wu et al., 2024). As indicated in Table 1, as the proportion of CEP increased, the amount of leaching of amylose gradually decreased, indicating that CEP inhibited the leaching of amylose. It is hypothesised that polysaccharides bind more water, thereby preventing the leaching of amylose from starch granules (Xie, Ying, & Huang, 2022). Previous studies have shown that the addition of *Anemarrhena asphodeloides* polysaccharide (AARP) to wheat starch also inhibits the leaching of amylose. The AARP adheres to leached amylose and surrounds the surface of starch granules, preventing further leaching of amylose (Zhu et al., 2022).

### 3.2. S and SP

S and SP can be used to characterise the extent of amylose leaching and the water absorption capacity of starch granules during the swelling process (Shi et al., 2023). As shown in Table 1, the solubility of CES-0% CEP was 6.33%, while the solubility of the CES-CEP complexes showed an increasing trend with the increase of CEP content. The solubility was 11.33% when the amount of CEP added was 1.5%. This may be due to the shear force or osmotic pressure exerted by CEP on the starch surface resulting in enlarged pore size of starch granules, increased water absorption, granule swelling and rupture, and exudation of amylose into the continuous phase during the pasting process (Zheng et al., 2024). The swelling power of CES-0.5%CEP, and CES-1.0%CEP were 10.69% and 10.83%, respectively, and the results of the significance analysis showed that, although the values decreased slightly, the introduction of low concentrations (0.5% and 1.0%) of CEP did not have a significant effect on the whole system ($p > 0.05$), and only when the addition amount of CEP reached 1.5%, the mixed system's swelling degree showed a significant increase. A plausible explanation may be that CEP can absorb water and enhance the water-holding capacity of the CES-CEP system. Li et al. (2019) had the same speculation about wheat starch in their study of *Artemisia sphaerocephala* Krasch polysaccharide.

### 3.3. Pasting properties

The pasting properties of starch reflect the ability of starch to absorb water and swell at high temperatures, which has an important influence on the quality of starch-based products. The pasting curves and the pasting parameters are presented in Fig. 1A and Table 1. From Table 1, it can be observed that the pasting temperatures of the complexes were continuously increased by the addition of CEP. This may be because CEP competes with starch for free water in the system and the swelling process of the starch paste granules is hindered.

Peak viscosity (PV) is the viscosity of starch granules when their volume expands to the maximum level during heating, indicating the degree of expansion of starch granules during the pasting process. The experimental results showed that the addition of CEP significantly reduced the PV of CES. It can be attributed to the adhesion of polysaccharides to the surface of starch granules, which inhibits starch swelling and leaching of amylose, thus reducing the overall viscosity of the system. On the other hand, CEP may penetrate the starch granules to form complexes, further reducing the water activity and inhibiting the

**Table 1**
S, SP, Leaching of amylose and pasting parameters of CES-CEP complexes.

| Samples | Leaching of amylose (%) | S (%) | SP (g/g) | PT (°C) | PV (BU) | BD (BU) | SB (BU) |
|---|---|---|---|---|---|---|---|
| CES-0%CEP | 11.63 ± 0.17$^{a}$ | 6.33 ± 1.04$^{c}$ | 13.37 ± 5.39$^{b}$ | 70.60 ± 0.10$^{b}$ | 372.50 ± 0.50$^{a}$ | 89.00 ± 6.00$^{a}$ | 220.00 ± 8.00$^{c}$ |
| CES-0.5%CEP | 11.05 ± 0.17$^{b}$ | 8.17 ± 0.76$^{bc}$ | 10.69 ± 0.44$^{b}$ | 70.95 ± 0.35$^{b}$ | 335.00 ± 17.00$^{b}$ | 62.50 ± 2.50$^{b}$ | 224.00 ± 3.00$^{bc}$ |
| CES-1.0%CEP | 11.00 ± 0.29$^{b}$ | 9.00 ± 0.87$^{b}$ | 10.83 ± 0.44$^{b}$ | 71.45 ± 0.05$^{a}$ | 325.33 ± 12.09$^{b}$ | 58.50 ± 6.50$^{b}$ | 236.00 ± 13.00$^{ab}$ |
| CES-1.5%CEP | 10.81 ± 0.17$^{b}$ | 11.33 ± 1.44$^{a}$ | 15.14 ± 0.84$^{a}$ | 71.75 ± 0.15$^{a}$ | 316.00 ± 7.00$^{b}$ | 58.50 ± 0.50$^{b}$ | 247.88 ± 1.50$^{a}$ |

Results are shown as mean values ± SD in triplicate. Values in the same columns showing the different letters are different significantly ($p < 0.05$). S, solubility. SP, swelling power. PT, pasting temperature. PV, peak viscosity. BD, breakdown. SB, setback.

expansion process of starch granules. This finding is consistent with previous studies on the effect of cellulase-assisted extraction of *Mesona chinensis* polysaccharides (MCP) on tapioca starch, and a similar decrease in viscosity was observed (Xiao et al., 2020). However, it is worth noting that the effects of polysaccharides obtained by different extraction methods on the viscosity of starch paste may be quite different. For example, Xiao et al. (2020) also found that MCP extracted with sodium carbonate increased the viscosity and the degree of recrystallization of the molecules after pasting. This phenomenon is mainly attributed to the association of starch paste, which may be related to the competitive water absorption between polysaccharides and starch and the formation of a rigid membrane structure.

The setback (SB) value is related to the recrystallization of amylose. The higher the SB, the easier the starch paste is retrograded (Kong et al., 2020). The addition of CEP in this study resulted in a significant increase in the SB value of CES. This may be due to the interaction of the amylose with polysaccharide during the dissolution process, which promotes the aggregation of dissolved and ruptured starch granules and the formation of a stronger gel network during the cooling process (Li et al., 2019). The enhanced stability of the complexes was also confirmed by the three-dimensional network structure formed by CEP and CES in the SEM image presented in Section 3.7. However, it is important to note that the effect of different polysaccharides on the starch paste regrowth values may differ significantly. For example, it has been shown that the addition of *Cordyceps* polysaccharide (CPS) reduces the SB value of wheat starch, which may be attributed to the intermolecular linkage between CPS and amylose, leading to the wrapping of CPS around the surface of starch granules and inhibiting the swelling and rupture of starch granules (Kong et al., 2020). This linkage may be stronger than the reaggregation of amylose, thus inhibiting the formation of the initial gel network structure and delaying the short-term ageing process.

The breakdown (BD) value can be used to evaluate the stability of starch granules in shear and thermal environments (Liu et al., 2018). It can be seen from the data in Table 1 that the BD value of the CES-CEP complexes was significantly reduced, indicating that the addition of CEP improved the thermal paste stability of starch. This may be due to the fact that polysaccharides are encapsulated on the starch surface, forming a protective film that effectively inhibits the swelling and fragmentation process of starch granules.

In food systems, the interactions between polysaccharides and starch usually involve electrostatic forces, hydrogen bonding, hydrophobic interactions, and van der Waals forces (Yang, Zhong, Douglas Goff, & Li, 2019). In this research system, the main components are CES and CEP, which are rich in hydroxyl groups in their chemical structure; therefore, hydrogen bonding and electrostatic forces are assumed to be the dominant interactions between them. To verify this hypothesis, two chemical reagents, NaCl and urea, can be added. NaCl would mainly interfere with the electrostatic interactions and have less effect on the hydrogen bonding. Urea, on the other hand, is a typical hydrogen bond breaker and has little effect on the electrostatic forces. The change in PV after the addition of NaCl and urea was determined by the Brabender viscometer. Fig. 1 demonstrates the pasting curves of CES-1.5%CEP complexes at different NaCl and urea concentrations. The results (Fig. 1B) showed that in the presence of NaCl, the degree of decrease in the PV value of the complexes was dependent on the concentration of NaCl. This phenomenon suggests that NaCl has a significant effect on the complexes during the formation or maintenance of the three-dimensional network structure of the system. Specifically, the electrostatic interaction between acidic polysaccharides in CEP and the sodium ions in NaCl exists. This shielding effect weakens the interaction between starch granules and polysaccharide molecules, resulting in the inability of starch granules to swell sufficiently and form a continuous network structure (Xie, Ren, Xiao, Luo, & Shen, 2021). The higher the concentration of NaCl, the more significant the decrease of PV, which is consistent with the findings of Su et al. (2024) in the Interaction force between laminarin and different crystal starches describes the gelatinization properties.

On the other hand, in the CES-1.5%CEP urea system (Fig. 1C), there was a slight decrease in the PV value of the complexes, which can be attributed to the disruptive effect of urea on the hydrogen bonding between starch molecules and polysaccharides. During the cooling process, the aggregation and rearrangement of starch were inhibited, resulting in increased fluidity between polymer molecular chains. This explanation is consistent with the Li, Wang, Chen, Liu, and Li (2017) report on the main force between corn starch and sodium alginate in their study and is consistent with the results of FTIR in Section 3.6. In summary, the interactions within the CES-CEP complexes are primarily governed by electrostatic interactions, with hydrogen bonding contributing to a lesser extent.

### 3.4. Rheological properties

The effect of CEP on the rheological properties of CES is exhibited in Fig. 1. As the shear rate increased, the samples exhibited a decrease in apparent viscosity (Fig. 1D) and a corresponding increase in shear stress (Fig. 1E). Notably, the CES-CEP complexes displayed rheological properties of shear thinning that are non-Newtonian. The introduction of CEP also affected the rheological properties of CES. Specifically, at low contents, the apparent viscosities of the CES-CEP complexes were consistently lower than those of CES-0%CEP. This may be due to the interaction of CEP with the amylose under electrostatic interaction, which inhibits the leaching of amylose. Additionally, polysaccharides were dispersed around the starch granules, reducing the water absorption capacity of starch granules. This, in turn, inhibited the swelling of starch granules, resulting in a decrease in the apparent viscosity of starch (Zheng et al., 2024). These findings are consistent with the analysis of swelling power results. Furthermore, it was observed that the apparent viscosity of CES-1.5%CEP was greater than that of CES-0% CEP, possibly due to an enhancement in viscosity resulting from the formation of a network structure between high contents of polysaccharide and starch (Han et al., 2022).

A power law equation (Ostwald) was used to fit the data, and the relevant parameters are shown in Table 2. The shear rate and shear stress exhibit high correlation coefficients ($R^2 > 0.99$), signifying a good fit with the power law model. The K decreased with the addition of CEP, further indicating that CEP reduced the viscosity of the complexes and enhanced their mobility. Comparable trends suggest a reduction in viscosity within the complexes and indicate that the introduction of polysaccharides hinders the leaching of amylose. The n of all samples ranged from 0.34 to 0.51 (all <1), indicating that all samples exhibited

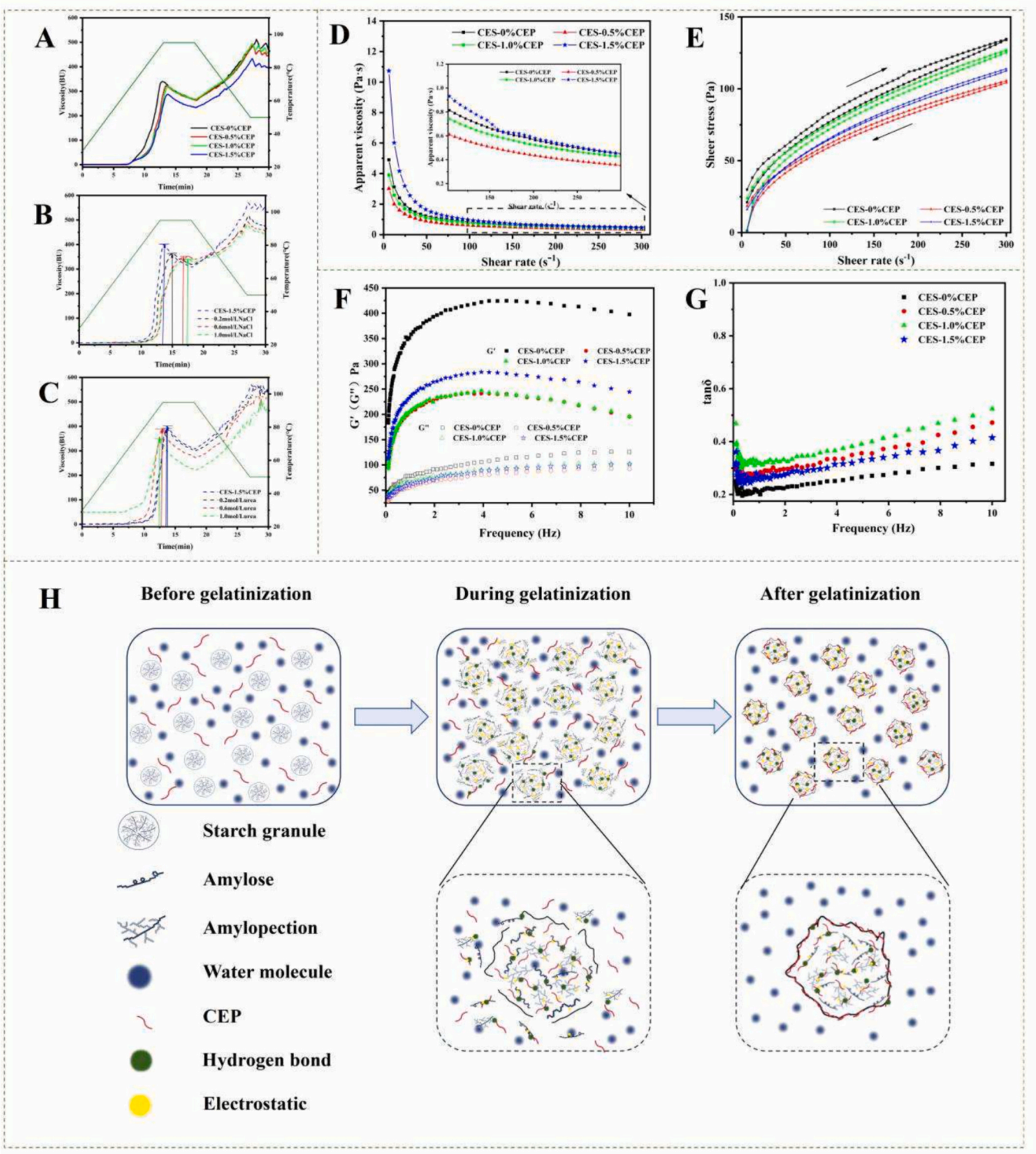


**Fig. 1.** Pasting curves and rheological properties of CES-CEP complexes.
Pasting curves of CES-CEP complexes (A). Pasting curves of CES-1.5%CEP complexes at different NaCl (B) and urea (C) concentrations. Sheer rate and apparent viscosity (D). Sheer rate and sheer stress (E). G', G" (F). tanδ (G).
The schematic diagram of the interaction mechanism between CEP and CES during the gelatinization process (H).

pseudoplastic fluids characteristics.

Thixotropy, a crucial rheological property, refers to the capacity of a water-soluble polymer solution to regain viscosity following external shear. When subjected to external shear, the apparent viscosity of starch changes to different degrees due to the disruption of its internal structure, exhibiting hysteresis loops of varying areas. Notably, a smaller thixotropic loop area indicates better viscosity retention. This loop area serves as a determinant for the energy required to disrupt the starch structure (Wu et al., 2024). Analysis of Table 2 reveals a significant reduction in the thixotropic loop area of the complexes with the addition of CEP. This suggests shorter recovery times and increased shear resistance, albeit without a consistent pattern with increasing CEP levels.

**Table 2**
Parameters for fitting the Ostwald equation for CES-CEP complexes.

| Samples | Upward Curve | | | Downward Curve | | | Hysteresis loops area (Pa·s) |
|---|---|---|---|---|---|---|---|
| | $K_1$ (Pa·s$^n$) | $n_1$ | $R_1^2$ | $K_2$ (Pa·s$^n$) | $n_2$ | $R_2^2$ | |
| CES-0% CEP | 18.93 ± 8.41$^a$ | 0.35 ± 0.08$^a$ | 0.99 | 11.57 ± 0.18$^a$ | 0.42 ± 0.01$^a$ | 0.99 | 2344.19 |
| CES-0.5% CEP | 10.11 ± 3.62$^a$ | 0.44 ± 0.03$^b$ | 0.99 | 9.97 ± 1.90$^a$ | 0.43 ± 0.01$^a$ | 0.99 | 547.09 |
| CES-1.0% CEP | 9.28 ± 2.59$^a$ | 0.44 ± 0.01$^b$ | 0.99 | 10.03 ± 0.28$^b$ | 0.43 ± 0.01$^a$ | 0.99 | 586.53 |
| CES-1.5% CEP | 8.77 ± 3.45$^a$ | 0.47 ± 0.06$^a$ | 0.99 | 10.30 ± 2.36$^b$ | 0.44 ± 0.01$^b$ | 0.99 | 302.13 |

Results are shown as mean values ± SD in triplicate. Values in the same columns showing the different letters are different significantly ($p < 0.05$).

This observation could be attributed to the enhancement of the three-dimensional structure of starch within the mixed systems (Wu et al., 2024).

The dynamic rheological properties of the CES-CEP complexes are presented in Fig. 1F. G′ and G″ represent the storage modulus and loss modulus of the samples, respectively. The loss factor (tanδ), which is the ratio of G″ to G′, provides insight into the material's state within a specific range (Liu et al., 2023). As evident in Fig. 1F, the addition of CEP led to a reduction in both G′ and G″ for the complexes compared to the control sample, CES-0%CEP. This reduction implies that CEP diminishes the elasticity of the pasted starch, making it behave more like a liquid than a solid. Furthermore, all CES-CEP complexes exhibited lower G″ values than CES-0%CEP, with an increasing trend observed for tanδ (Fig. 1G). These observations suggest that the incorporation of polysaccharides somewhat inhibited the binding between starch granules during the initial stages of starch gel setback, resulting in a more fluid-like behaviour (Zheng et al., 2024). As the testing frequency increased, both G′ and G″ values gradually rose. Notably, within the measured frequency range, G′ values were consistently higher than G″, indicating that the CES-CEP complexes displayed characteristic weak gel rheological behaviour (Ma et al., 2019). This could be attributed to the fact that the polysaccharide coating around most starch granules prevented the dispersion of amylose in the continuous phase, thereby reducing amylose-amylose interactions and impeding the formation of elastic gels (Kong et al., 2020).

### 3.5. LF-NMR analysis

Starch retrogradation is accompanied by moisture migration and redistribution, and LF-NMR is a rapid and convenient method for analysing moisture distribution in food systems (Zhou et al., 2022). This technique characterises the mobility of water molecules in food systems by measuring transverse relaxation time ($T_2$). The $T_2$ value effectively represents the motion status of water molecules, where a shorter $T_2$ value indicates tighter binding to the matrix and weaker mobility (Zhou et al., 2021). The change in the $T_2$ of CES under the influence of CEP is shown in Fig. 2A. With the increasing concentration of CEP in the system, the $T_2$ of the CES-CEP system exhibits a trend of first increasing and then decreasing. When the addition of CEP reaches 1.0%, the $T_2$ attains its shortest value (637.04 ms), indicating the greatest restriction on water molecule migration within the system. This may be attributed to the electrostatic interaction between high concentrations of CEP and leached amylose, promoting the formation of a more compact and ordered gel network structure, which binds more free water within the gel network. This observation is corroborated by the uniform "honeycomb" microstructure of the CES-1.0%CEP blend observed in the SEM analysis (Section 3.7).

### 3.6. FTIR

Fig. 2B illustrates the FTIR spectra of CES-CEP complexes and CEP. It can be observed that the absorption peaks near 3400 cm$^{-1}$ indicate the stretching vibration of the O—H group. The characteristic absorption peaks of polysaccharides were observed near 2930 cm$^{-1}$, while 1655 cm$^{-1}$ represents the asymmetric absorption peak of the C═O bond, and 1417 cm$^{-1}$ is the absorption peak of the C—H bond (Yu et al., 2023). Within the range of 4000–400 cm$^{-1}$, the shapes and positions of the infrared absorption peaks of the different complexes are very similar, with no emergence of new peaks or disappearance of characteristic peaks. The absence of significant peak shifts suggests that no new groups were formed within the system. Pronounced absorption peaks observed around 3400, 2930, and 1643 cm$^{-1}$ were attributed to the stretching vibration of -OH, the stretching vibration of -$CH_2$ and the O—H bending vibration of the bound water in the samples, respectively. In addition, the absorption peaks located near 1154, 1080, 1037 and 900 cm$^{-1}$ were identified as typical characteristic absorption peaks of sugar rings (Han et al., 2022).

To further investigate the impact of CEP addition on the short-range ordered structure of the samples, the 1200–800 cm$^{-1}$ band of the original infrared spectrum was subjected to deconvolution analysis. The changes in the ordered structure of starch are commonly analysed using

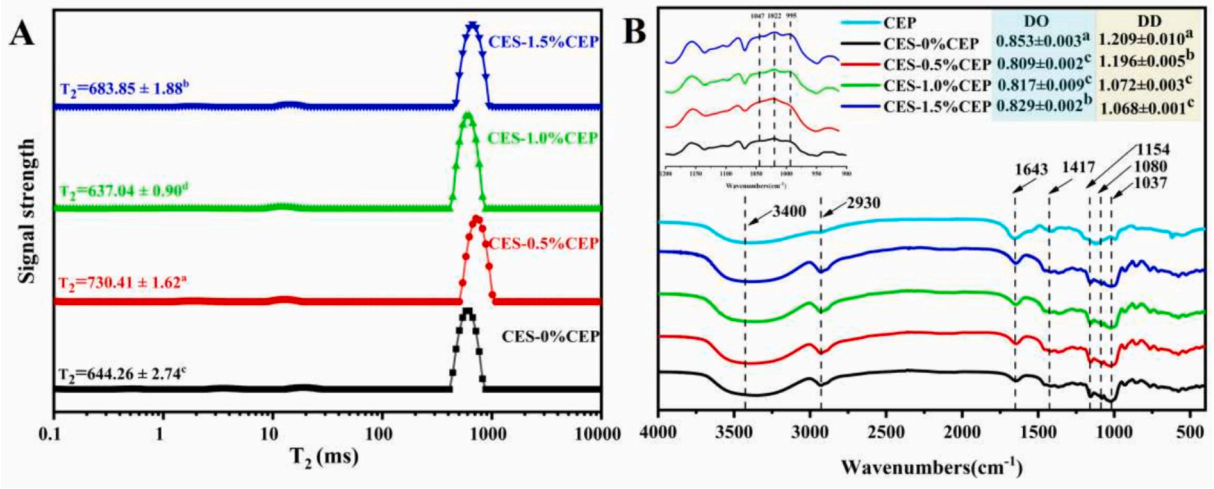


**Fig. 2.** Transverse relaxation time distribution and FTIR spectra of CES-CEP complexes.

the $R_{1047/1022}$ ratio (DO) and the $R_{1022/995}$ ratio (DD) (Wang et al., 2022). DO values serve as an indicator of the degree of starch short-range ordering, while DD values are associated with the extent of the double helix. Compared with CES-0%CEP, the DO values decreased with the addition of CEP, indicating that CEP effectively reduced the crystallinity of the samples. This suggests that polysaccharides in the system effectively inhibited the ordered rearrangement of starch molecular chains during cold storage of the starch paste (Zheng et al., 2019). With the addition of CEP, the DD values of the complexes gradually decreased. It indicated that CEP partially destroyed the original double helix structure of starch. The decrease in DD value also implies that the ageing of starch was promoted (Zhao, Jin, Wu, & Chen, 2023), which is consistent with the viscosity test results. Zhou et al. (2021) found that the DO value and DD value of *Auricularia auricula-judae* polysaccharide (AAJP)-kidney bean starch (KBST) gels were significantly increased after the addition of AAJP in the study of AAJP-KBST complexes, resulting in AAJP promoted the formation of a solid ordered structure and a more compact double helix structure of KBST.

### 3.7. SEM

Fig. 3 demonstrates the SEM image of the cross-section of the freeze-dried CES-CEP complexes. After the complexes were pasted, the granular structure of the native starch was disrupted, resulting in the rearrangement of amylose, amylopectin, and CEP within CES during the cooling process. As evident in Fig. 3A, the CES-0%CEP complexes exhibit a rough, irregular grid structure characterised by large pores and thick walls. With increasing CEP addition, significant morphological changes were observed in the complexes. CES-0.5%CEP displayed a parallel lamellar structure, likely attributed to increased entanglement between starch fragments and CEP, which generates a repulsive force that separates water from the homogeneous gel phase (Liu et al., 2019). The microstructure of the CES-1.0%CEP complexes exhibited a uniform "honeycomb" shape. Studies have demonstrated that hydrogen bonding interaction between polysaccharides and starch granules can promote water separation and alter the pore count in starch gels (Luo et al., 2020). The CES-1.5%CEP complexes feature a network sheet structure supported by mutual cross-linking. This structure is attributed to the aggregative and entangling effects of CEP with leached amylose. Specifically, CEP forms a viscous phase around solubilized starch granules, disrupting the starch network through interactions with amylose. The interplay between CEP and amylose diminishes the interactions among amylose chains, thereby disrupting the starch network and leading to the formation of network lamellae (Jia et al., 2023).

### 3.8. In vitro digestibility

The digestion of starchy foods in humans is intimately linked to postprandial blood glucose and insulin levels, with the rate of hydrolysis playing a key role in this response (Chen et al., 2019). Fig. 4 illustrates the impact of varying CEP additions on the *in vitro* digestion of CES. As seen from Fig. 4A, the enzymatic rate of starch digestion exhibits three distinct phases. In the initial phase (0–20 min), there is a notable increase in the rate of amylase digestion, leading to a pronounced glycemic response. This is followed by a second phase (20–120 min) where the digestion rate stabilizes, resulting in a reduced glycaemic response. Finally, in the third phase (after 120 min), the rate of amylase digestion reaches equilibrium, implying that it no longer influences the glycaemic response. Notably, these three stages are consistent with the categorization of starch as rapidly digestible starch (RDS), slowly digestible starch (SDS), and resistant starch (RS) by Englyst and Hudson (1996).

As evident in Fig. 4B, the introduction of CEP had a pronounced impact on the RDS, SDS, and RS composition of the samples,

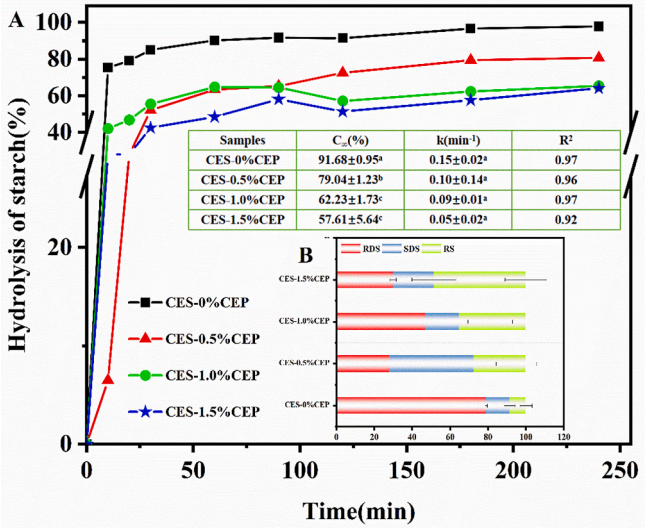


**Fig. 4.** Effect of CEP on the *in vitro* digestion of CES.

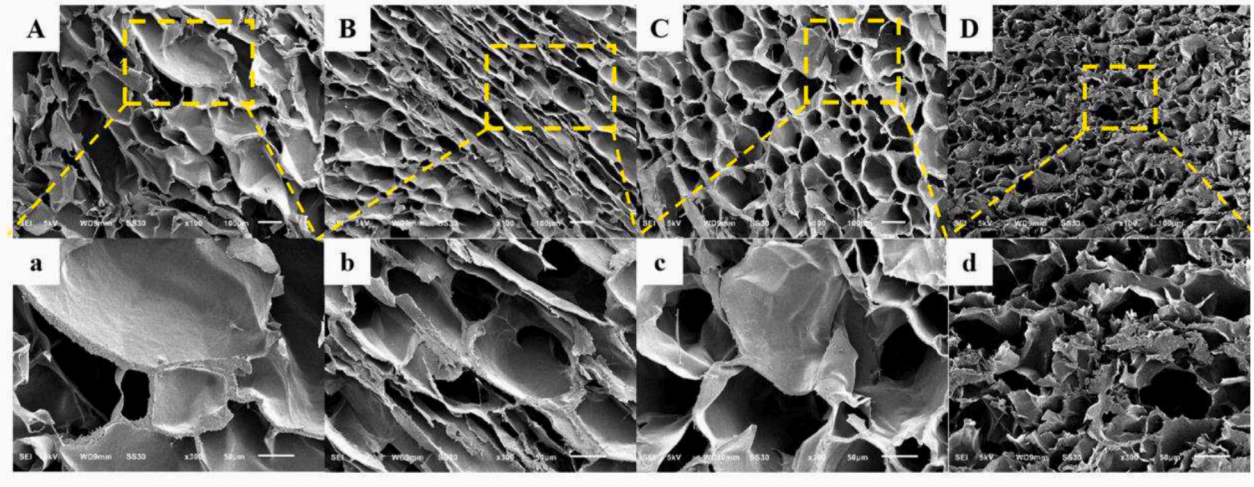


**Fig. 3.** SEM of CES-CEP complexes.
A-D: CES-0%CEP, CES-0.5%CEP, CES-1.0%CEP, CES-1.5%CEP (100×).
a-d: CES-0%CEP, CES-0.5%CEP, CES-1.0%CEP, CES-1.5%CEP (300×).

demonstrating a strong content-dependent inhibition of digestion. Specifically, the RDS constituent of the CES-CEP complexes underwent a drastic reduction from 79.15% to 29.85% with the increasing CEP content. Conversely, both the SDS (12.31%–21.61%) and RS (8.54%–48.53%) components experienced notable increases. These findings indicate that the incorporation of CEP significantly hindered starch digestibility, thereby contributing to the moderation of postprandial blood glucose and insulin levels.

A plausible explanation for this observation is that the encapsulation of polysaccharides forms a protective barrier on the outside of the starch granules under electrostatic, which reduces the accessibility of digestive enzymes to the starch substrate. Furthermore, the intermolecular interactions between polysaccharides and starch result in an augmentation of the system's viscosity, which in turn restricts water mobility and diminishes the diffusion and release of hydrolysis byproducts (Zhou et al., 2021). In comparison, CEP fractions are comprised of not only α-D-Glucose but also β-D-Glucose, β-D-Galactose, α-D-Xylose, and cellulose polysaccharides (Wang et al., 2023). The presence of these additional components may have further influenced the digestibility of CES. Previous literature has also demonstrated that non-starch polysaccharides in mushroom polysaccharides can interfere with the digestion of sorghum starch, exerting a mild inhibitory effect (Tu et al., 2023). Furthermore, *Lentinus edodes* β-glucan has also been shown to interfere with the digestion of wheat starch (Zhuang et al., 2017). To assess the impact of CEP on the digestibility of CES-CEP complexes, *in vitro* digestibility curves were subjected to first-order kinetic fitting. This analysis allowed for the calculation of $C_\infty$ and k for the samples, with the results presented in Fig. 4. Notably, all samples exhibited an $R^2$ value >0.9, indicating a strong fit to the starch digestibility curve. The addition of CEP had a profound influence on the *in vitro* digestibility of the CES-CEP complexes. Specifically, as the CEP content increased from 0% to 1.5%, the $C_\infty$ of the complexes gradually decreased, suggesting a negative correlation between $C_\infty$ and CEP content. This observation can be attributed to the fact that the incorporation of polysaccharides alters the structure of the starch gel, thereby inhibiting amylase activity and reducing starch digestibility (Zheng et al., 2024). In terms of starch digestion rate constants, a clear trend was observed: $k_{CES\text{-}0\%CEP} > k_{CES\text{-}0.5\%CEP} > k_{CES\text{-}1.0\%CEP} > k_{CES\text{-}1.5\%CEP}$. This trend can be explained by the fact that polysaccharides reduce the amount of leached amylose during starch pasting. Additionally, CEP interacts with the leached amylose, further slowing down the hydrolytic action of the enzyme (Shi et al., 2023).

### 3.9. Mechanism diagram of the interaction between CES and CEP

The mechanism underlying the interaction between CEP and CES during the pasting process is illustrated in Fig. 2H. During starch pasting, polysaccharides engage with water molecules and starch, modulating the physicochemical properties of starch. Starch granules are composed of amylose and amylopectin. Amylose is composed of D-Glucose units linked *via* α-1,4 glycosidic bonds, resulting in a helical conformation. In contrast, the amylopectin molecule exhibits a combination of α-1,6 and α-1,4 glycosidic bonds, leading to the formation of branches.

Before pasting, starch exists in a granular state. When CEP is added at proportions ranging from 0.5% to 1.5%, it coats the surface of the starch granules through electrostatic interactions and hydrogen bonding, which impede the interaction between the starch granules and water molecules and suppress the leaching of amylose (Table 1). As the pasting process begins, the starch granules undergo absorption of water and subsequent swelling. During this phase, CEP competes with starch for water molecules, retarding the swelling of the starch granules. This interference leads to an increase in pasting temperature and a decrease in PV for the CES-CEP complexes compared to the CES-0%CEP control sample (Table 1). Once the starch granules have completely broken down, CEP becomes uniformly distributed within the fragmented starch, serving as a diluent and enhancing the flow of starch paste fragments under shear (Fig. 1E). During the cooling process of the starch paste, under electrostatic interactions, CEP entangles and rearranges with both amylose and amylopectin *via* hydrogen bonding, resulting in an intertwined mesh structure. This mesh structure acts as a bridging agent, enhancing the strength of the starch gel. Evidence of this can be observed through SEM of CES-1.5%CEP samples (Fig. 3).

## 4. Conclusions

The present study concludes that varying amounts of CEP significantly influence the pasting properties, rheological properties, and *in vitro* digestibility of CES. The inclusion of CEP resulted in a decreasing trend in both the peak viscosity and breakdown value of the CES-CEP complexes. In contrast, the heat stability of the starch pastes was augmented. Rheologically, the CES-CEP complexes paste exhibited pseudoplastic fluid characteristics, manifesting a distinctive weak gel rheological behaviour. Furthermore, CEP coating on the starch surface formed a physical barrier, reducing the accessibility of digestive enzymes to the starch substrate and consequently decreasing starch digestibility. As a functional ingredient, CEP can improve the processing characteristics of food products to a certain extent. The present study offers fundamental insights into the effects of CEP on the properties of starch-based food products and contributes to the understanding of the intricate interactions between starch and polysaccharide macromolecules.

## CRediT authorship contribution statement

**Xiuli Wu:** Conceptualization, Supervision, Writing – review & editing, Funding acquisition. **Qing Zhang:** Methodology, Formal analysis, Data curation, Writing – original draft. **Jianwen Zhang:** Data curation, Visualization. **Bingqian Zhang:** Software, Validation. **Xuexu Wu:** Data curation, Software. **Xiangxuan Yan:** Validation, Visualization.

## Declaration of competing interest

The authors declare no conflict of interest.

## Data availability

Data will be made available on request.

## Acknowledgements

This research was supported by the Enterprise Commissioned Technology Development Program (2023JBH26L50).

## Appendix A. Supplementary data

Supplementary data to this article can be found online at https://doi.org/10.1016/j.fochx.2024.101511.

## References

Builders, P. F., Anwunobi, P. A., Mbah, C. C., & Adikwu, M. U. (2013). New direct compression excipient from tiger nut starch: Physicochemical and functional properties. *AAPS PharmSciTech, 14*(2), 818–827. https://doi.org/10.1208/s12249-013-9968-7

Chen, L., Tian, Y., Tong, Q., Zhang, Z., & Jin, Z. (2017). Effect of pullulan on the water distribution, microstructure and textural properties of rice starch gels during cold storage. *Food Chemistry, 214*, 702–709. https://doi.org/10.1016/j.foodchem.2016.07.122

Chen, L., Zhang, H., McClements, D. J., Zhang, Z., Zhang, R., Jin, Z., & Tian, Y. (2019). Effect of dietary fibers on the structure and digestibility of fried potato starch: A comparison of pullulan and pectin. *Carbohydrate Polymers, 215*, 47–57. https://doi.org/10.1016/j.carbpol.2019.03.046

Englyst, H. N., & Hudson, G. J. (1996). The classification and measurement of dietary carbohydrates. *Food Chemistry, 57*(1), 15–21. https://doi.org/10.1016/0308-8146(96)00056-8

Han, X., Wen, H., Luo, Y., Yang, J., Xiao, W., & Xie, J. (2022). Effects of chitosan modification, cross-linking, and oxidation on the structure, thermal stability, and adsorption properties of porous maize starch. *Food Hydrocolloids, 124*, Article 107288. https://doi.org/10.1016/j.foodhyd.2021.107288

Hernández-Olivas, E., Asensio-Grau, A., Calvo-Lerma, J., García-Hernández, J., Heredia, A., & Andrés, A. (2022). Content and bioaccessibility of bioactive compounds with potential benefits for macular health in tiger nut products. *Food Bioscience, 49*, Article 101879. https://doi.org/10.1016/j.fbio.2022.101879

Huang, J., Yu, M., Wang, S., & Shi, X. (2023). Effects of jicama (*Pachyrhizus erosus* L.) non-starch polysaccharides with different molecular weights on structural and physicochemical properties of jicama starch. *Food Hydrocolloids, 139*, Article 108502. https://doi.org/10.1016/j.foodhyd.2023.108502

Jia, S., Tao, H., Zhao, H., Yu, B., Wu, Z., Liu, P., & Cui, B. (2023). Effects of *Lycium barbarum* polysaccharide on pasting, rheology, and *in vitro* digestibility of starch. *Starch/Stärke, 75*(1–2), 2200185. https://doi.org/10.1002/star.202200185

Jia, S., Yu, B., Zhao, H., Tao, H., Liu, P., & Cui, B. (2022). Physicochemical properties and *in vitro* digestibility of dual-modified starch by cross-linking and annealing. *Starch - Stärke, 74*(1–2), 2100102. https://doi.org/10.1002/star.202100102

Kong, X.-R., Zhu, Z.-Y., Zhang, X.-J., & Zhu, Y.-M. (2020). Effects of *Cordyceps* polysaccharides on pasting properties and *in vitro* starch digestibility of wheat starch. *Food Hydrocolloids, 102*, Article 105604. https://doi.org/10.1016/j.foodhyd.2019.105604

Li, Q.-Q., Wang, Y.-S., Chen, H.-H., Liu, S., & Li, M. (2017). Retardant effect of sodium alginate on the retrogradation properties of normal cornstarch and anti-retrogradation mechanism. *Food Hydrocolloids, 69*, 1–9. https://doi.org/10.1016/j.foodhyd.2017.01.016

Li, X., Li, J., Yin, X., Wang, X., Ren, T., Ma, Z., Li, X., & Hu, X. (2019). Effect of *Artemisia sphaerocephala* Krasch polysaccharide on the gelatinization and retrogradation of wheat starch. *Food Science & Nutrition, 7*(12), 4076–4084. https://doi.org/10.1002/fsn3.1273

Liu, H.-M., Miao, W.-B., Wang, R., Chen, N., Ma, S.-Y., & Wang, X.-D. (2021). Improvement of functional and rheological features of tigernut tuber starch by using gum derived from Chinese quince seeds. *LWT, 143*, Article 111180. https://doi.org/10.1016/j.lwt.2021.111180

Liu, Q., Chen, P., Li, P., Zhao, J., Olnood, C. G., Zhao, S., … Chen, X. (2023). Effects of Salecan on the gelatinization and retrogradation behaviors of wheat starch. *LWT-Food Science and Technology, 186*, Article 115238. https://doi.org/10.1016/j.lwt.2023.115238

Liu, S., Lin, L., Shen, M., Wang, W., Xiao, Y., & Xie, J. (2018). Effect of *Mesona chinensis* polysaccharide on the pasting, thermal and rheological properties of wheat starch. *International Journal of Biological Macromolecules, 118*, 945–951. https://doi.org/10.1016/j.ijbiomac.2018.06.178

Liu, S., Xiao, Y., Shen, M., Zhang, X., Wang, W., & Xie, J. (2019). Effect of sodium carbonate on the gelation, rheology, texture and structural properties of maize starch-*Mesona chinensis* polysaccharide gel. *Food Hydrocolloids, 87*, 943–951. https://doi.org/10.1016/j.foodhyd.2018.09.025

Luo, Y., Xiao, Y., Shen, M., Wen, H., Ren, Y., Yang, J., Han, X., & Xie, J. (2020). Effect of *Mesona chinensis* polysaccharide on the retrogradation properties of maize and waxy maize starches during storage. *Food Hydrocolloids, 101*, Article 105538. https://doi.org/10.1016/j.foodhyd.2019.105538

Ma, S., Zhu, P., Wang, M., Wang, F., & Wang, N. (2019). Effect of konjac glucomannan with different molecular weights on physicochemical properties of corn starch. *Food Hydrocolloids, 96*, 663–670. https://doi.org/10.1016/j.foodhyd.2019.06.014

Shi, X., Yu, M., Yin, H., Peng, L., Cao, Y., & Wang, S. (2023). Multiscale structures, physicochemical properties, and *in vitro* digestibility of oat starch complexes co-gelatinized with jicama non-starch polysaccharides. *Food Hydrocolloids, 144*, Article 108983. https://doi.org/10.1016/j.foodhyd.2023.108983

Su, J., He, S., Lei, S., Huang, K., Li, C., Zhang, Y., & Zeng, H. (2024). Interaction force between laminarin and different crystal starches describes the gelatinization properties. *Food Hydrocolloids, 147*, Article 109380. https://doi.org/10.1016/j.foodhyd.2023.109380

Tu, J., Adhikari, B., Brennan, M. A., Cheng, P., Bai, W., & Brennan, C. S. (2023). Interactions between sorghum starch and mushroom polysaccharides and their effects on starch gelatinization and digestion. *Food Hydrocolloids, 139*, Article 108504. https://doi.org/10.1016/j.foodhyd.2023.108504

Wang, H., Yuan, M., Li, G., Tao, Y., Wang, X., Ke, S., Zhuang, M., Wang, A., & Zhou, Z. (2023). Chemical characterization, antioxidant and immunomodulatory activities of acetylated polysaccharides from *Cyperus esculentus*. *Food Chemistry, 427*, Article 136734. https://doi.org/10.1016/j.foodchem.2023.136734

Wang, L., Zhu, L., Gao, J., Zhang, F., Li, L., Yang, Y., & Xu, Y. (2022). Effect of dandelion root polysaccharide on structure, rheology and retrogradation properties of corn starch during storage. *International Journal of Food Science & Technology, 57*(10), 6522–6530. https://doi.org/10.1111/ijfs.15991

Wu, X., Luan, M., Yan, X., Zhang, J., Wu, X., & Zhang, Q. (2024). The impact of different concentrations of hyaluronic acid on the pasting and microstructural properties of corn starch. *International Journal of Biological Macromolecules, 254*, Article 127555. https://doi.org/10.1016/j.ijbiomac.2023.127555

Xiao, Y., Liu, S., Shen, M., Jiang, L., Ren, Y., Luo, Y., & Xie, J. (2020). Effect of different *Mesona chinensis* polysaccharides on pasting, gelation, structural properties and *in vitro* digestibility of tapioca starch-*Mesona chinensis* polysaccharides gels. *Food Hydrocolloids, 99*, Article 105327. https://doi.org/10.1016/j.foodhyd.2019.105327

Xie, H., Ying, R., & Huang, M. (2022). Effect of arabinoxylans with different molecular weights on the gelling properties of wheat starch. *International Journal of Biological Macromolecules, 209*, 1676–1684. https://doi.org/10.1016/j.ijbiomac.2022.04.104

Xie, J., Ren, Y., Xiao, Y., Luo, Y., & Shen, M. (2021). Interactions between tapioca starch and *Mesona chinensis* polysaccharide: Effects of urea and NaCl. *Food Hydrocolloids, 111*, Article 106268. https://doi.org/10.1016/j.foodhyd.2020.106268

Yang, C., Zhong, F., Douglas Goff, H., & Li, Y. (2019). Study on starch-protein interactions and their effects on physicochemical and digestible properties of the blends. *Food Chemistry, 280*, 51–58. https://doi.org/10.1016/j.foodchem.2018.12.028

Yu, T., Wu, Q., Wang, J., Liang, B., Wang, X., & Shang, X. (2023). Physicochemical properties of tiger nut (*Cyperus esculentus* L) polysaccharides and their interaction with proteins in beverages. *Food Chemistry: X, 19*, Article 100776. https://doi.org/10.1016/j.fochx.2023.100776

Zhang, R.-Y., Huang, X.-Y., Chen, P.-X., Li, T., Jiang, M.-M., Wang, Y.-L., Zhu, W.-X., & Liu, H.-M. (2023). A novel non-centrifugal sugar prepared from tiger nut (*Cyperus esculentus* L.) meal: Preparation methods and comparison with sugarcane. *Food Research International, 174*, Article 113519. https://doi.org/10.1016/j.foodres.2023.113519

Zhao, L., Jin, X., Wu, J., & Chen, H. (2023). Effects of *Qingke* β-glucan with different molecular weights on pasting, gelation, and digestive properties of rice starch. *Food Chemistry: X, 19*, Article 100803. https://doi.org/10.1016/j.fochx.2023.100803

Zheng, J., Wang, N., Yang, J., You, Y., Zhang, F., Kan, J., & Wu, L. (2024). New insights into the interaction between bamboo shoot polysaccharides and lotus root starch during gelatinization, retrogradation, and digestion of starch. *International Journal of Biological Macromolecules, 254*, Article 127877. https://doi.org/10.1016/j.ijbiomac.2023.127877

Zheng, M., You, Q., Lin, Y., Lan, F., Luo, M., Zeng, H., Zheng, B., & Zhang, Y. (2019). Effect of guar gum on the physicochemical properties and *in vitro* digestibility of lotus seed starch. *Food Chemistry, 272*, 286–291. https://doi.org/10.1016/j.foodchem.2018.08.029

Zhou, J., Jia, Z., Wang, M., Wang, Q., Barba, F. J., Wan, L., … Fu, Y. (2022). Effects of Laminaria japonica polysaccharides on gelatinization properties and long-term retrogradation of wheat starch. *Food Hydrocolloids, 133*, Article 107908. https://doi.org/10.1016/j.foodhyd.2022.107908

Zhou, R., Wang, Y., Wang, Z., Liu, K., Wang, Q., & Bao, H. (2021). Effects of *Auricularia auricula-judae* polysaccharide on pasting, gelatinization, rheology, structural properties and *in vitro* digestibility of kidney bean starch. *International Journal of Biological Macromolecules, 191*, 1105–1113. https://doi.org/10.1016/j.ijbiomac.2021.09.110

Zhu, L., Zhang, F., Yang, Y., Liang, X., Shen, Q., Wang, L., & Xu, Y. (2022). Extraction, purification, structural characterization of *Anemarrhena asphodeloides* polysaccharide and its effect on gelatinization and digestion of wheat starch. *Industrial Crops and Products, 189*, Article 115867. https://doi.org/10.1016/j.indcrop.2022.115867

Zhuang, H., Chen, Z., Feng, T., Yang, Y., Zhang, J., Liu, G., Li, Z., & Ye, R. (2017). Characterization of *Lentinus edodes* β-glucan influencing the *in vitro* starch digestibility of wheat starch gel. *Food Chemistry, 224*, 294–301. https://doi.org/10.1016/j.foodchem.2016.12.087